

# Adaptive Air-to-Ground Secure Communication System based on ADS-B and Wide Area Multilateration

Yogesh Nijsure<sup>†</sup>, Member, IEEE, Georges Kaddoum, Member, IEEE, Ghyslain Gagnon, Member, IEEE, Francois Gagnon, Member, IEEE, Chau Yuen, Senior Member, IEEE and Rajarshi Mahapatra, Member, IEEE

<sup>†</sup> Corresponding author, e-mail: y.nijsure.2014@ieee.org

**Abstract**—A novel Air-to-Ground (ATG) communication system, based on adaptive modulation and beamforming enabled by Automatic Dependent Surveillance-Broadcast (ADS-B) and multilateration technique is presented in this work. From an aircraft geolocation perspective, the proposed multilateration technique uses the Time-Difference-of-Arrival (TDOA), Angle-of-Arrival (AOA), and Frequency-Difference-of-Arrival (FDOA) features within the ADS-B signal to implement the hybrid geolocation mechanism. Moreover, this hybrid mechanism aims at the optimal selection of multilateration sensors to provide a precise aircraft geolocation estimate by minimizing the Geometric Dilution of Precision (GDOP) metric and also imparts significant resilience to the current ADS-B based geolocation framework to withstand any form of attack involving aircraft-impersonation and ADS-B message infringement. From an ATG communication perspective, the ground Base Stations (BSs) can use this hybrid aircraft geolocation estimate to dynamically adapt their modulation parameters and transmission beampattern, in an effort to provide a high data rate secure ATG communication link. Additionally, we develop a hardware prototype which is highly accurate in estimating the AOA data and facilitating TDOA, FDOA extraction associated with the received ADS-B signal. This hardware setup for the ADS-B based ATG system is analytically established and validated with commercially available universal-software-defined-radio-peripheral (USRP) units. This hardware setup displays a 1.5° AOA estimation accuracy, whereas the simulated geolocation accuracy is approximately 30 m over 100 nautical miles for a typical aircraft trajectory. The adaptive modulation and beamforming approach assisted by the proposed GDOP minimization based multilateration strategy achieves significant enhancement in throughput and reduction in packet error rate.

**Index Terms**—ADS-B Multilateration, Air-to-Ground Communication, Adaptive Modulation, Hybrid Geolocation, in-flight broadband, AOA estimation.

## I. INTRODUCTION

In-flight broadband services and on-board cellular connectivity for commercial airlines has given rise to satellite-based in-flight connectivity for transcontinental flights [1].

Copyright (c) 2015 IEEE. Personal use of this material is permitted. However, permission to use this material for any other purposes must be obtained from the IEEE by sending a request to [pubs-permissions@ieee.org](mailto:pubs-permissions@ieee.org).

Yogesh Nijsure, Georges Kaddoum, Ghyslain Gagnon, and Francois Gagnon are with University of Québec, ETS, 1100 Notre-Dame west, H3C 1K3, Montreal, Canada (e-mail: [y.nijsure.2014@ieee.org](mailto:y.nijsure.2014@ieee.org); [georges.kaddoum@etsmtl.ca](mailto:georges.kaddoum@etsmtl.ca); [Ghyslain.Gagnon@etsmtl.ca](mailto:Ghyslain.Gagnon@etsmtl.ca); [Francois.Gagnon@etsmtl.ca](mailto:Francois.Gagnon@etsmtl.ca)). Chau Yuen is with Singapore University of Technology and Design, Singapore (email: [yuenchau@sutd.edu.sg](mailto:yuenchau@sutd.edu.sg)). Rajarshi Mahapatra is with the Graphic Era University, India (email: [rajarshim@ieee.org](mailto:rajarshim@ieee.org)).

Intercontinental flights cover huge distances involving oceans, deserts, and polar remote airspace, hence the usage of satellites seems to be a natural choice for such an application. The usage of a satellite-based architecture, however, poses constraints with respect to the cost and achievable data rate for the overall system [1]–[3]. Thus, for continental flights, the Air-to-Ground (ATG) framework emerges as a better choice. This architecture employs several ground-based base stations (BSs) or cellular networks to provide the ATG communication link with the aircraft. Some of the examples of ATG service providers include Aircell and Gogo in-flight internet in U.S.A. Currently, Aircell and Gogo provide in-flight internet service for domestic flights for continental U.S. flights through cellular network of over a 100 ground stations [4].

Several network architectures have been proposed in the literature describing in-flight broadband applications [1], [2], [5], which include multi-hop *ad hoc* networking between aircrafts. Such a multihop architecture forms a new communication scenario involving ground stations and satellites, known as the aeronautical *ad hoc* network (AANET) [1]. AANET is a new *ad hoc* network between commercial aircrafts in the sky for the purpose of sharing of data and internet access. AANET describes an *ad hoc* network in which the ground stations, satellites, and aircrafts collaborate to provide internet access over flights. Such collaboration can be facilitated by exchanging data between aircrafts through single hop or multiple hop networking [1]. However the current data rates offered by such service providers remain restricted to 3.1–9 Mbps [6], mainly due to the nature of the ATG channel, which is subject to significant Doppler shift, path-loss, and interference constraints [4]. Specifically, Gogo provides in-flight internet service data rate upto 10 Mbps, based on their second generation ATG-4 systems. Future ATG systems will adopt a hybrid Ground-To-Orbit (GTO) framework which combines current ATG-4 and Ku-band satellite based infrastructures. These hybrid systems can offer data-rates in excess of 60 Mbps, however ATG-4 systems are still preferred due to their relatively low cost, simple and quicker installation requirements [6], [7].

In this work, we focus on enhancing the performance of current ATG-4 type systems, by adopting the proposed ATG framework. To this end, we need a highly accurate real-time geolocation estimation of the aircraft. This can be achieved using the Automatic Dependent Surveillance Broadcast (ADS-B) technique [8]. Current aircraft surveillance techniques

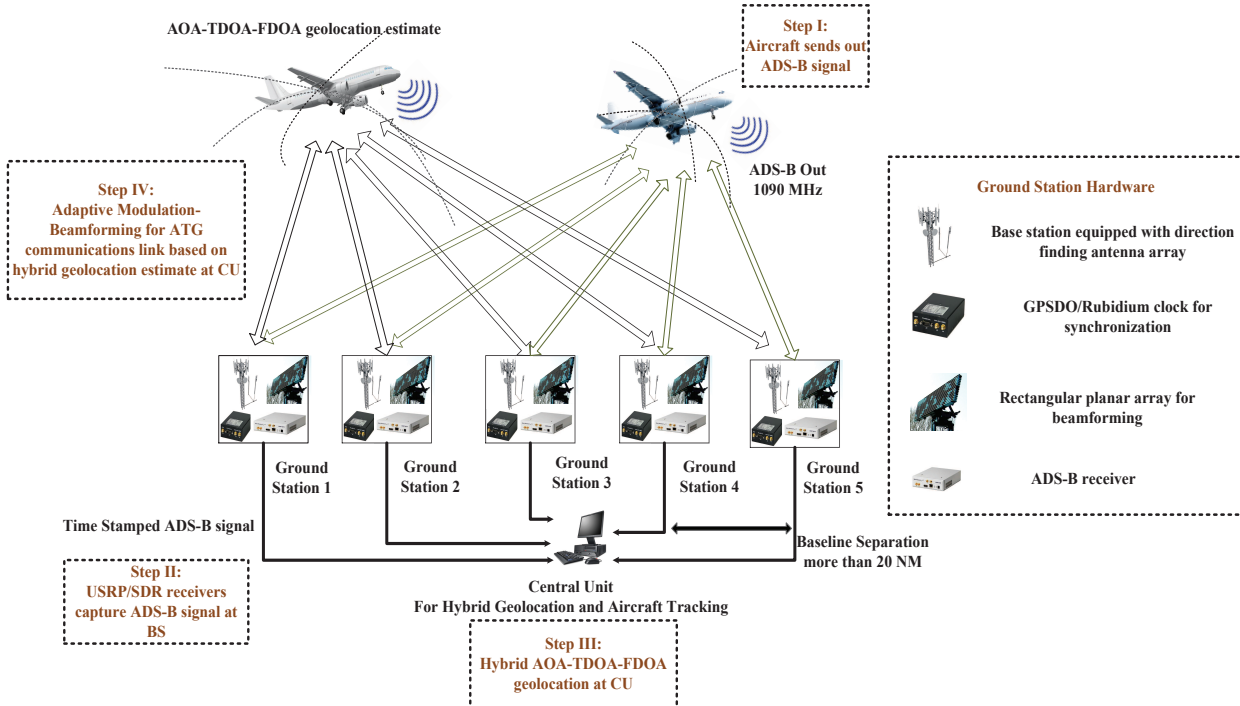


Fig. 1. Proposed system architecture.

involve the use of Primary Surveillance Radar (PSR) and Secondary Surveillance Radar (SSR), which are to be replaced by the ADS-B technology by the end of year 2025 [8]. Low cost ADS-B 1090 MHz receivers for personal use are available on the market, and can be connected to a standard computer. The ADS-B technology has been conceived to be an un-authenticated and un-encrypted signal to allow open and free visibility to all aircrafts within the airspace. Thus, the current implementation of ADS-B signal suffers from the following security vulnerabilities [8] including (i) Lack of data authentication to protect against message injection from unauthorized entities, and (ii) Absence of message encryption to protect against eavesdropping, and aircraft impersonation.

Several approaches to overcome these shortcomings have been discussed in the literature [9]–[15]. Approaches mentioned in [13]–[15] suggest estimating the Angle-of-Arrival (AOA) of the ADS-B signal. One of these approaches also includes the implementation of ADS-B systems coupled with Wide Area Multilateration (WAMLAT), which relies upon capturing the ADS-B signal over widely separated sensors in order to allow aircraft location estimation which can be independent of the conventional ADS-B signal demodulation. ADS-B transponders, when coupled with the multilateration technique, can offer a much more reliable and cost-effective option for addressing the needs of future Air Traffic Management (ATM) systems. It is expected that WAMLAT coupled with ADS-B will support existing SSR infrastructure on airports. WAMLAT systems rely on the deployment of sensors over a wide area to facilitate the Time-of-Arrival (TOA), and Time-Difference-of-Arrival (TDOA) schemes for aircraft geolocation. The TDOA-assisted WAMLAT system, coupled

with ADS-B, can provide a far more accurate estimate of the location of the aircraft, compared to PSR or SSR, and is cost-effective [8], [11]. This significantly improves aircraft tracking and detection performance over the SSR architecture [11], [16]–[18].

#### *Key Motivation for the proposed approach:*

Existing state-of-the-art technology to enable ATG-4 type systems [6], [7], can benefit from the real-time aircraft tracking enabled by ADS-B based geolocation. More recent works like [19] have highlighted the necessity of addition of more resilient mechanisms in addition to ADS-B based geolocation. The main focus of our work is based on improving the current ATG set-up for transcontinental flights by introducing a novel WAMLAT architecture for optimal sensor selection based on Geometric Dilution of Precision (GDOP) minimization, which not only alleviates the current ADS-B message infringement threats but also allows accurate geolocation even though the integrity of the ADS-B message is compromised.

Moreover, the adaptive modulation and beamforming approach for ATG system facilitated by the proposed novel WAMLAT approach can provide a secure point-to-point ATG link with the individual aircrafts and thus can offer similar communications performance as compared to an ATG system which relies on an un-spoofed ADS-B signal. This research is aimed at enhancing the security and data rate performance of the ATG-4 type infrastructure provided by the in-flight broadband service providers like Aircell and Gogo.

The major contributions of this proposed research can be summarized as follows:

- Development of novel a AOA-TDOA-Frequency Difference of Arrival (FDOA) based framework which aims

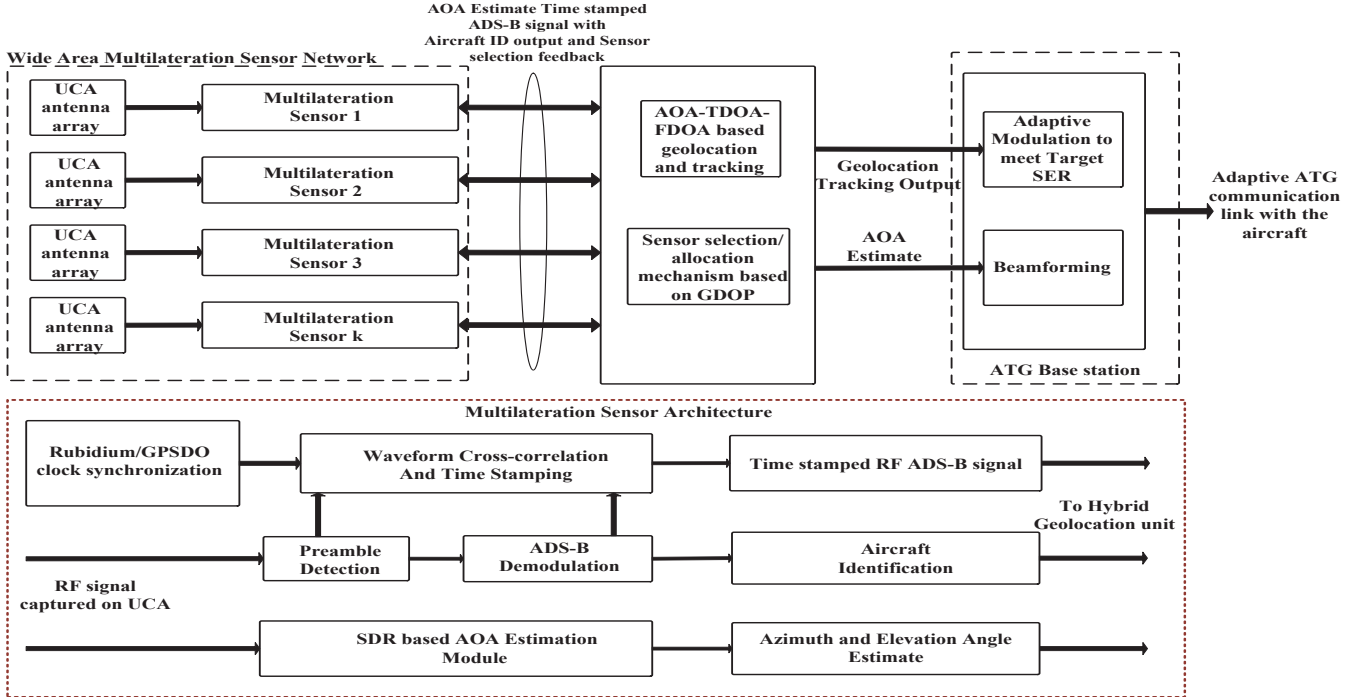


Fig. 2. Proposed ATG communications approach.

at optimal selection of multilateration sensors based on minimizing the GDOP and provides additional safeguards for handling ADS-B security threats and aircraft discrimination.

- Realization of ATG communications system enabled by ADS-B multilateration. Specifically, we develop an adaptive modulation and beamforming mechanism based on real-time position information, to establish a high quality of service, secure ATG communications link.
- Implementation of a software-defined-radio based hardware prototype for facilitating AOA-TDOA-FDOA and ADS-B signal acquisition.

The rest of the paper is organized as follows. In Section II, we provide a general overview of the proposed ATG communication system architecture. In Section III, we present the actual GDOP minimization based multilateration mechanism for aircraft tracking in real-time, in Section IV the adaptive modulation and beamforming approach for the ground-based cellular BSs is presented. Simulation and experimental results are described in detail in Section V, which show the efficiency of the proposed adaptive modulation and beamforming approach enabled by the ADS-B multilateration technique. Finally, in Section VI, we provide concluding remarks and potential applications.

## II. SYSTEM ARCHITECTURE

A general system architecture for the proposed ATG communication coupled with the ADS-B multilateration technique for aircraft surveillance is shown in Fig. 1.

We assume that the cellular BSs are scattered over a wide area to provide the ATG communications link with the aircraft as shown in Fig. 1. The system comprises ATG BSs and randomly deployed multilateration sensor units which maintain a dedicated link with the ATG BSs. The proposed system mechanism shown in Fig. 1 can be broken down into 4 steps. It is assumed that the aircraft is equipped with an ADS-B transponder and it continually transmits the ADS-B signal at 1090 MHz every second. This ADS-B signal is a 120  $\mu$ sec Pulse Position Modulated (PPM) signal, containing the aircraft relevant information in terms of its identity, altitude, GPS location, barometric pressure, bearing, etc.

The second step involves the capture of this ADS-B signal frame on antenna arrays stationed at each of the multilateration units. This signal can be acquired on any commercially available Software-Defined-Radio (SDR) receiver like the Universal Software Defined Radio Peripheral (USRP) unit. It is assumed that all the SDR receivers are synchronized by a common GPS Disciplined Oscillator (GPSDO)/rubidium clock standard to assist synchronous capture of the ADS-B frames. In addition to the data acquisition SDR receivers, we also utilize a novel hardware prototype for estimating the AOA of the ADS-B signal in azimuth and elevation angles. In step 3, we estimate the aircraft geolocation within the 3D space around the base station by utilizing the AOA-TDOA-FDOA features within the ADS-B signals. In addition to this, we also identify the most optimal set of multilateration units to be utilized depending on the hybrid geolocation estimate. This optimal selection of multilateration sensors is an attempt to minimize GDOP and maximize the accuracy of geolocation

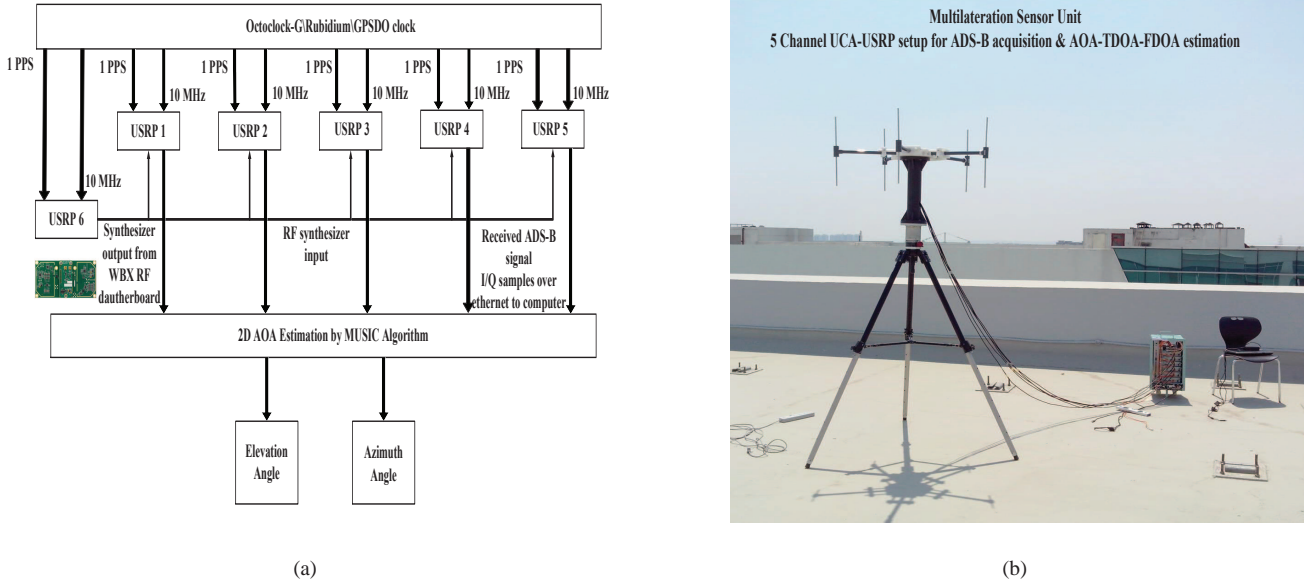


Fig. 3. (a) AOA estimation hardware setup at a particular sensor node, (b) Multilateration sensor unit hardware setup.

estimate even if the ADS-B signal is compromised. Finally, in step 4, this hybrid geolocation estimate is used to assist the proposed adaptive modulation and beamforming mechanism at the BS, in an effort to enhance the quality of service of the ATG communication link.

As mentioned earlier, we present a novel hardware setup to deduce the AOA of the ADS-B signal, which will assist our proposed AOA-TDOA-FDOA based hybrid geolocation. This hardware setup can be integrated with the existing ADS-B infrastructure at the multilateration unit. As shown in Fig. 2, we assume that the BSs are scattered over a WAMLAT units are randomly deployed. In particular, we use the USRP units for ADS-B signal acquisition for facilitating the proposed AOA estimation to assist AOA-TDOA-FDOA hybrid geolocation. The motivation behind the use of USRP units is their low cost and compatibility with standard signal processing software. The hardware implementation is based on ADS-B signal acquisition from USRP units is described in detail in Section III-A. As seen from Fig. 2, a particular multilateration sensor architecture consists of ADS-B signal acquisition unit, ADS-B preamble detection and captured RF time-stamping facilitated by a Rubidium/GPSDO clock standard. Moreover the sensor unit comprises of the SDR based hardware prototype to estimate the AOA of the acquired signal. This time-stamped RF ADS-B signal along with the AOA estimates from all the multilateration units is sent to a Central Unit (CU) for TDOA/FDOA profile computation. The CU then performs the hybrid AOA-TDOA-FDOA geolocation algorithm and implements the proposed GDOP minimization algorithm to select the most optimal set of sensor units based on the current aircraft track. This geolocation fix established from the most optimal set of sensor units is relayed to

the ATG base station to allow the adaptive modulation and beamforming mechanism.

#### A. GDOP based WAMLAT strategy

GDOP is a vital metric which indicates the efficacy of the sensor network topological distribution in aiding multilateration as mentioned in works like [20], [21]. As shown in Fig. 2, for a particular spatial distribution of multilateration sensor units, the achieved GDOP value refers to the dilution in precision of the aircraft position estimate. Our main intention within the proposed WAMLAT strategy is to identify the most optimal spatial distribution of sensor units which can provide a high geolocation accuracy. Additionally, this proposed WAMLAT framework utilizes AOA-TDOA-FDOA features within the captured ADS-B signal at the optimally distributed sensor units.

As mentioned in Section I, the ADS-B signal is vulnerable to message infringement and spoofing attacks. These modes of attack will affect the geolocation estimation if we solely rely upon the demodulation of the ADS-B frame for computing the location, velocity, and other relevant information for the aircraft. In order to circumvent these issues, we utilize the ADS-B signal in its raw RF form without demodulating it to achieve AOA-TDOA-FDOA based multilateration. Since we intend on extracting and utilizing additional features such as AOA-TDOA-FDOA within the acquired ADS-B frame, it becomes virtually impossible for any ground based-attacker or a malicious transmission source to "mimic" the authentic ADS-B signal. Specifically, we extract the TDOA and FDOA profiles of the ADS-B signal by capturing synchronously the ADS-B signal on multiple SDR receivers deployed at the widely scattered WAMLAT units. The timing synchronization

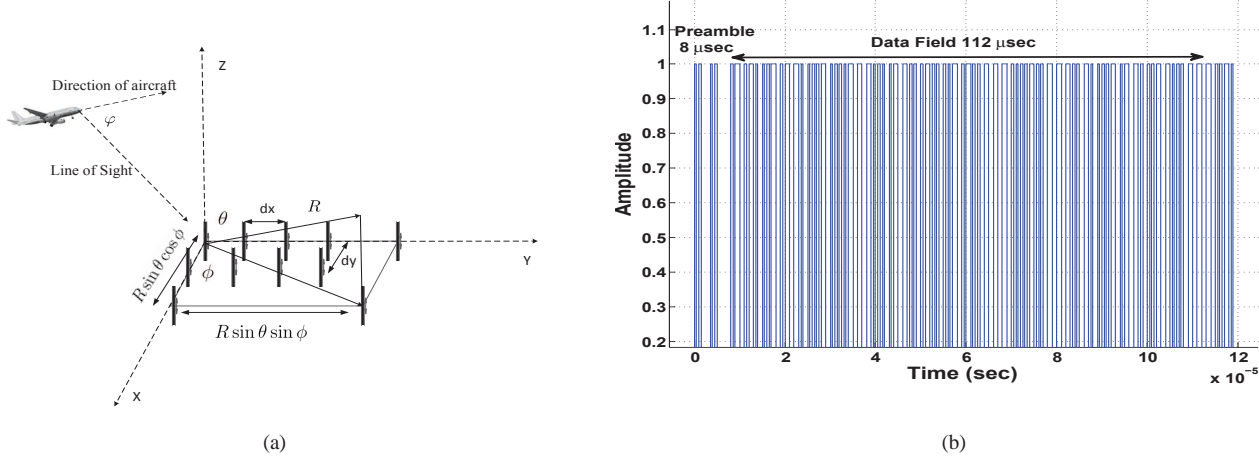


Fig. 4. (a) Rectangular antenna array geometry for beamforming, (b) Transmitted ADS-B signal from the aircraft transponder.

between the SDR units at each WAMLAT unit is provided by the rubidium/GPSDO clocks, which can provide a timing accuracy of the order of 20 ns [22]. By utilizing our AOA estimation hardware setup we further improve our TDOA-FDOA based geolocation estimate by fusing the extracted AOA feature. This refines the geolocation estimate, which can then be fused with the demodulated position information of the aircraft, to provide a reliable and secure geolocation track of the aircraft.

#### B. Adaptive Modulation and Beamforming at the BS

Based on the 3D geolocation estimate of the aircraft generated by the GDOP minimization based WAMLAT approach, each BS can ascertain the real-time distance to the aircraft and determine the optimal modulation scheme to be utilized for enhancing the data-rate for the ATG communication link. Moreover, this geolocation estimate could improve the quality of service for the ATG communication link by adopting a beamforming solution at the BS. The choice of the modulation scheme is influenced by the maximum achievable Signal to Noise Ratio (SNR) at the aircraft, which in turn depends upon the current distance between the aircraft and the BS, whereas, the beamforming mechanism aims at reducing the interference for a multi-aircraft scenario and providing a directional secure link with the aircraft. In this work, we assume that the base stations equipped with ADS-B receivers have a dominant Line-of-Sight (LOS) component with the aircraft. Such an assumption results in a Rician fading channel [23], [24] for the ATG communication link as well as the ADS-B link.

It is important to note that for the AOA-TDOA-FDOA based multilateration system, we do not intend to demodulate the ADS-B signal to achieve the hybrid geolocation, hence the performance of the hybrid geolocation mechanism does not degrade severely due to the Rician fading channel. However, the ATG communication link is affected by the path-loss and

Rician fading channel and, is analyzed separately in this work. This will be described in detail in Section IV.

### III. GDOP BASED AOA-TDOA-FDOA MULTILATERATION STRATEGY

As shown in Fig. 2, ADS-B receivers on the ground are equipped with Uniform Circular Array (UCA) to capture the ADS-B signal for TOA, FOA, and AOA estimation. We also assume that the aircrafts operate in ADS-B out mode and that the ground receivers capture the 1090 MHz ADS-B squitter. These parameters are passed on to the CU for extraction of the TDOA-FDOA profile, along with the AOA estimates. The mechanism for this overall system is initiated with the capture of the ADS-B signal on the antenna array.

#### A. AOA estimation hardware prototype

We propose an AOA estimation hardware setup, which can be easily integrated with the existing WAMLAT infrastructure to facilitate ADS-B signal acquisition and AOA estimation required for the proposed AOA-TDOA-FDOA based hybrid geolocation. As shown in Fig. 3(a) and Fig. 3(b), we use the UCA configuration of dipole elements connected to USRP units to capture synchronously the ADS-B signal being transmitted from the aircraft transponder. This subsystem computes the 2D AOA by adopting the MUSIC and ESPRIT algorithms in [25] to compute the azimuth and elevation angles from the captured ADS-B signals.

The hardware setup in Fig. 3(a) shows a mechanism to achieve synchronization in ADS-B signal acquisition across different USRP units and its integration with the 2D AOA estimation algorithm. We interface the USRP units [26] with a standard MATLAB/SIMULINK platform in order to process the captured ADS-B signal and deduce the AOA data. The exact hardware implementation has been explained in detail

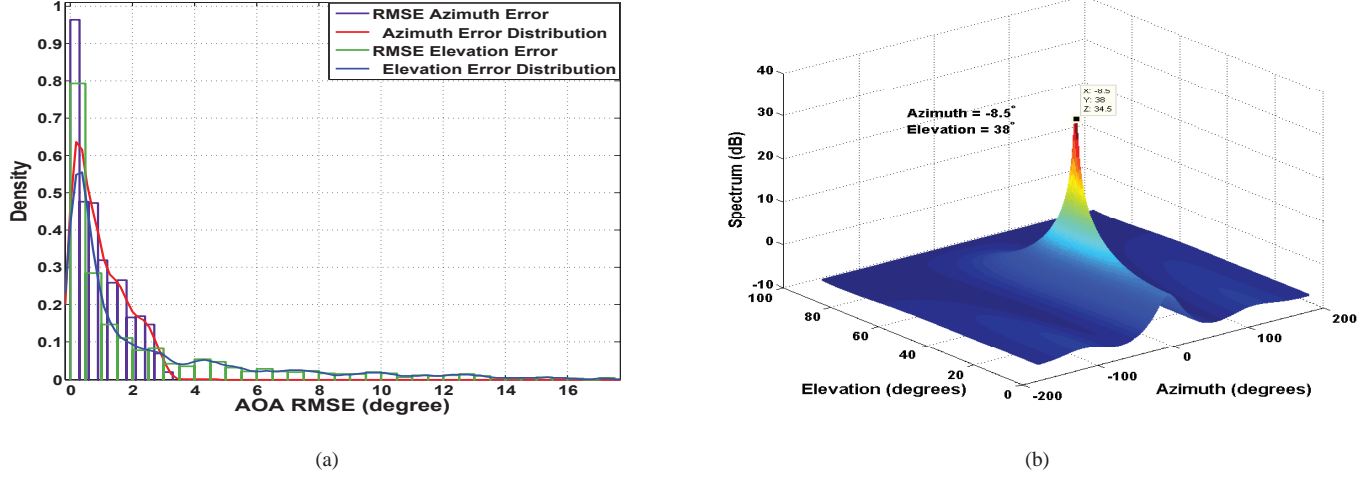


Fig. 5. (a) Practical result: Estimated AOA error distribution for the USRP based UCA hardware prototype, (b) Simulation based 2D AOA estimation through UCA-RB-MUSIC algorithm at each WAMPLAT sensor unit.

in Section V-A. Upon AOA estimation, GPS time vector is appended to the captured ADS-B signal at all the ADS-B ground stations, and the captured and time-stamped ADS-B signals are sent to the CU for TDOA/FDOA processing. At the CU, the time-stamps are aligned to cross-correlate the signals and compute the time-difference profiles to enable TDOA computation. The AOA estimation module at each ADS-B ground station will also relay the azimuth  $\phi$  and elevation  $\theta$  angles to the CU to form the hybrid optimization problem for aircraft geolocation.

#### B. Hybrid AOA-TDOA-FDOA based Geolocation and Tracking

The mechanism for computing the joint AOA-TDOA-FDOA hybrid algorithm can be described as follows:

Let  $\vec{r}_i$  be the range vector between the ADS-B station  $i$  and the aircraft;  $\{x_a, y_a, z_a\}$  be the current position of the aircraft;  $\|\vec{v}_a\| = \sqrt{v_{x_a}^2 + v_{y_a}^2 + v_{z_a}^2}$  be the aircraft speed, where  $\{v_{x_a}, v_{y_a}, v_{z_a}\}$  are the component speeds in the  $x, y, z$  directions respectively; and  $\{x_i, y_i, z_i\}$  be the position of the ADS-B station.

$$\|\vec{r}_i\| = \sqrt{(x_a - x_i)^2 + (y_a - y_i)^2 + (z_a - z_i)^2}. \quad (1)$$

The TDOA between sensor  $i$  and sensor 1 is then defined by  $\Delta\tau_{i,j}$

$$\Delta\tau_{i,1} = \tau_i - \tau_1 + \eta_{\Delta\tau_{i,1}} = \frac{1}{c}(\|\vec{r}_i\| - \|\vec{r}_1\|) + \eta_{\Delta\tau_{i,1}}, \quad (2)$$

where  $c$  is the speed of light, and TDOAs are assumed to be obtained with respect to first sensor,  $\eta_{\Delta\tau_{i,1}}$  is the noise associated with  $\Delta\tau_{i,1}$  and the index  $i$  runs from 2 to  $k$ .

The non-linear relationship between the received signal AOAs and the emitter/sensor co-ordinates is expressed as follows:

$$\phi'_i = \phi_i + \eta_\phi, \quad (3)$$

$$\theta'_i = \theta_i + \eta_\theta. \quad (4)$$

where  $\phi_i = \tan^{-1}\left(\frac{y_a - y_i}{x_a - x_i}\right)$ ,  $\theta_i = \tan^{-1}\left(\frac{z_a - z_i}{\sqrt{(x_a - x_i)^2 + (y_a - y_i)^2}}\right)$  and  $\phi'_i$ ,  $\theta'_i$  are corresponding noisy measurements. A similar AOA estimation problem was addressed in [27, (13)], we adopt this set of AOA system of equations for the  $k^{th}$  sensor which can be expressed as

$$-(x_a - x_k) \sin \phi_k / \xi_{k,1} + (y_a - y_k) \cos \phi_k / \xi_{k,1} = 0 \\ -(x_a - x_k) \sin \theta_k / \xi_{k,2} \cos \phi_k + (z_a - z_k) \cos \theta_k / \xi_{k,2} = 0 \quad (5)$$

where  $\xi_{k,1} = \sqrt{(x_a - x_k)^2 + (y_a - y_k)^2}$  and  $\xi_{k,2} = \sqrt{(x_a - x_k)^2 + (y_a - y_k)^2 + (z_a - z_k)^2}$ .

In this work, we adopt the well known UCA-Real Beamspace MUSIC (UCA-RB-MUSIC) and UCA-ESPRIT algorithms found in [25]. The estimates for the azimuth angle  $\phi$  and the elevation angle  $\theta$  are computed from the UCA-RB-MUSIC algorithm. The mathematical formulation of these algorithms is beyond the scope of this discussion, but can be found in [25].  $\eta_\theta$  and  $\eta_\phi$  are the associated noise variables with the elevation and azimuth angle estimates respectively. Equations (3) and (4) represent the estimated AOA, whereas the hardware setup described in Section III-A which uses the UCA-RB-MUSIC algorithm as mentioned in [25] serves as the observed AOA. The performance of the proposed hardware setup for AOA estimation is described in detail in Section V.

Owing to the velocity of the aircraft relative to the ADS-B ground sensor, a change in frequency, or Doppler shift, occurs. If the aircraft is moving directly towards or away from the sensor, the observed FOA  $f_i^{obs}$  of the signal at the ADS-B sensor is:

$$f_i^{obs} = \left[ 1 + \frac{\vec{r}_i \cdot \vec{v}_{a,i}}{c \|\vec{r}_i\|} \right] f^o = \left[ 1 + \frac{\|\vec{v}_{a,i}\|}{c} \cos(\varphi_i) \right] f^o, \quad (6)$$

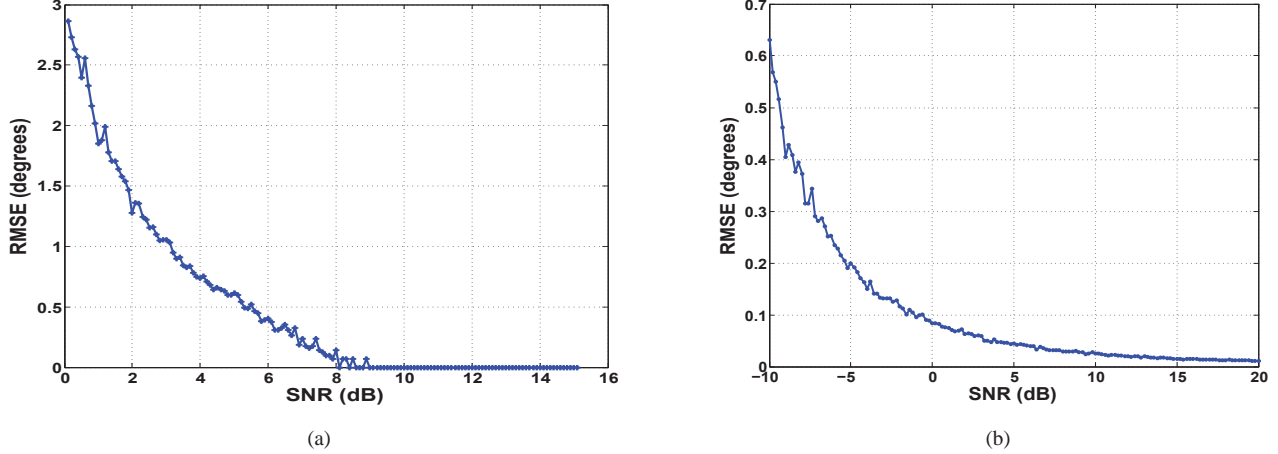


Fig. 6. (a) RMSE performance for the 2D AOA estimation for UCA-RB-MUSIC algorithm [25], (b) RMSE performance for the 2D AOA estimation for UCA-ESPRIT algorithm [25].

where  $\vec{v}_{a,i}$  represents the relative velocity of the aircraft with respect to sensor  $i$ . The center frequency  $f^o = 1090$  MHz, and  $\varphi_i$  is the angle between the LOS from the aircraft and the direction of the movement of the aircraft relative to the ADS-B station as shown in Fig. 4(a).

The FDOA at two different ADS-B ground stations  $\{i, j\}$  can be defined by

$$\Delta f_{i,j} = \frac{f^o}{c} \left[ \frac{\vec{r}_i \cdot \vec{v}_{a,i}}{\|\vec{r}_i\|} - \frac{\vec{r}_j \cdot \vec{v}_{a,j}}{\|\vec{r}_j\|} \right] + \eta_{f_{i,j}}, \quad (7)$$

where  $\eta_{f_{i,j}}$  is the associated noise component of the measured FDOA. As derived in [27, (15)] the hybrid system can be modelled as

$$\mathbf{m} = \mathbf{g}(\Psi) + \eta, \quad (8)$$

where  $\Psi = [x_a, y_a, z_a, v_{x_a}, v_{x_b}, v_{x_z}]^T$  is the vector of unknown variables,

$$\mathbf{m} = [\Delta\tau_{2,1}, \dots, \Delta\tau_{k,1}, 0, 0, \dots, 0, \Delta f_{2,1}, \dots, \Delta f_{k,1}]^T \quad (9)$$

From (2), (5), (7), (8), and (9) we can express the hybrid system as follows,

$$\mathbf{g}(\Psi) = \begin{bmatrix} (\|\vec{r}_2\| - \|\vec{r}_1\|)/c \\ \vdots \\ (\|\vec{r}_k\| - \|\vec{r}_1\|)/c \\ -(x_a - x_1)\sin\phi_1/\xi_{k,1} + (y_a - y_1)\cos\phi_1/\xi_{k,1} \\ -(x_a - x_1)\sin\theta_1/\xi_{k,2}\cos\phi_1 + (z_a - z_1)\cos\theta_1/\xi_{k,2} \\ \vdots \\ -(x_a - x_k)\sin\phi_k/\xi_{k,1} + (y_a - y_k)\cos\phi_k/\xi_{k,1} \\ -(x_a - x_k)\sin\theta_k/\xi_{k,2}\cos\phi_k + (z_a - z_k)\cos\theta_k/\xi_{k,2} \\ \frac{f^o}{c} \left( \frac{\vec{r}_2 \cdot \vec{v}_{a,2}}{\|\vec{r}_2\|} - \frac{\vec{r}_1 \cdot \vec{v}_{a,1}}{\|\vec{r}_1\|} \right) \\ \vdots \\ \frac{f^o}{c} \left( \frac{\vec{r}_k \cdot \vec{v}_{a,k}}{\|\vec{r}_k\|} - \frac{\vec{r}_1 \cdot \vec{v}_{a,1}}{\|\vec{r}_1\|} \right) \end{bmatrix} \quad (10)$$

The hybrid AOA-TDOA-FDOA estimation problem can be expressed as follows,

$$\hat{\Psi} = \min_{\Psi} \|(\mathbf{m} - \mathbf{g}(\Psi))\|, \quad (11)$$

where  $\hat{\Psi}$  is the hybrid estimate of the aircraft location and velocity. Equation (11) can be solved using least squares minimization algorithms, such as the Levenberg-Marquardt algorithm [27]. The observations  $\hat{\Psi}$ , and a state-model  $\Psi$  can be utilized to implement a standard linear KF for trajectory tracking as shown in works like [28], [29].

### C. GDOP based Multilateration Sensor Allocation Mechanism

As mentioned in [8], [30], ADS-B based aircraft geolocation presents a very accurate geolocation estimate, provided it is not “spoofed”. In this work we present additional safeguards to counter the spoofing and ADS-B message infringement threats by relying upon a fusion based solution enabled by multilateration and ADS-B. As shown in [8], the multilateration mechanism does not match the accuracy provided by an unspoofed ADS-B signal due to multiple reasons like, level of available synchronization between sensor nodes, placement of sensors within the wide area multilateration network, system latency in TDOA based estimation, etc. Out of these mentioned problems we address the sensor dynamic allocation/selection problem to enhance the multilateration performance. This novel technique is based on enhancing the performance of the multilateration based mechanism by minimizing the GDOP which is a vital parameter which degrades the multilateration performance.

A higher GDOP value for a particular topological distribution of the sensor networks represents poor multilateration performance. Hence an optimization algorithm is necessary

TABLE I  
ADS-B LINK BUDGET

Transmitter Characteristics	air-to-air	air-to-ground	air-to-air	air-to-ground
Frequency (MHz)	1090	1090	1090	1090
<b>Power (W)</b>	<b>125.00</b>	<b>125.00</b>	<b>125.00</b>	<b>125.00</b>
Power (dBm)	50.97	50.97	50.97	50.97
Antenna Gain (dBi)	0.00	0.00	7.00	7.00
VSWR	2.00	2.00	2.00	2.00
VSWR Loss (dB)	0.51	0.51	0.51	0.51
Cable and Connector Loss (dB)	1.00	1.00	1.00	1.00
<b>EIRP (dBm)</b>	<b>49.46</b>	<b>49.46</b>	<b>56.46</b>	<b>56.46</b>
Channel Characteristics				
<b>Link Range (nmi)</b>	<b>18</b>	<b>9</b>	<b>80</b>	<b>50</b>
Free Space Path Loss (dB)	123.64	117.62	136.60	132.52
O2 Absorption (dB)	0.05	0.07	0.25	0.38
Path Average Rainfall Rate (mm/hour)	0	0	0	0
Rainfall Absorption (dB)	0.00	0.00	0.00	0.00
Excess Path Loss (dB)	0.00	6.00	0.00	6.00
<b>Total Path Loss (dB)</b>	<b>123.70</b>	<b>123.69</b>	<b>136.85</b>	<b>138.90</b>
Receiver Characteristics	air-to-air	air-to-ground	air-to-air	air-to-ground
Antenna Gain (dB)	0.00	0.00	7.00	7.00
VSWR	2.00	2.00	2.00	2.00
VSWR Loss (dB)	0.51	0.51	0.51	0.51
Cable and Connector Loss (dB)	1.00	1.00	1.00	1.00
Receiver Noise Figure	5.00	5.00	5.00	5.00
Implementation Loss (dB)	1.00	1.00	1.00	1.00
Equivalent Receiver Noise at Antenna Input (dBm/Hz)	-168.74	-168.74	-175.74	-175.74
Environmental Noise (dBm/Hz)	-184.00	-184.00	-184.00	-184.00
<b>Environmental Plus Equivalent Receiver Noise (dBm/Hz)</b>	<b>-168.62</b>	<b>-168.62</b>	<b>-175.14</b>	<b>-175.14</b>
Received Signal				
<b>C/No (dB-Hz)</b>	<b>94.38</b>	<b>94.38</b>	<b>94.75</b>	<b>92.70</b>
Channel Burst Bit Rate (kHz)	20000	20000	20000	20000
Code Rate	1/2	1/2	1/2	1/2
Information Bit Rate (kHz)	10000.00	10000.00	10000.00	10000.00
Eb/No Available (dB)	23.38	23.38	23.75	21.70
Eb/No Required (dB)	2.60	2.60	2.60	2.60
<b>Link Margin (dB)</b>	<b>20.78</b>	<b>20.78</b>	<b>21.15</b>	<b>19.10</b>

to determine the best set of multilateration sensors to be utilized to aid the geolocation of the aircraft trajectory. This optimization or selection of randomly distributed multilateration sensors would be dynamic and dependent on the current aircraft trajectory estimate generated by the linear KF and (11).

In order to derive the GDOP minimization problem, for a single aircraft ADS-B source and  $k = 2$  sensor nodes, we define the AOA-TDOA-FDOA profile  $\Upsilon(\mathbf{X})$  as a function of actual position  $\mathbf{X} = [x, y, z]^T$ , the measured AOA-TDOA-FDOA profile as  $\mathbb{M}$  and corresponding noise vector  $\eta$ . We assume that the aircraft has a constant velocity with respect to the  $X$ ,  $Y$  and  $Z$  axes. Thus for the case of  $k = 2$  sensor nodes,

$$\Upsilon(\mathbf{X}) = \begin{bmatrix} \Delta\tau'_{2,1} \\ \phi_1 \\ \theta_1 \\ \phi_2 \\ \theta_2 \\ \Delta f'_{2,1} \end{bmatrix} = \begin{bmatrix} (\|\vec{r}_2\| - \|\vec{r}_1\|)/c \\ \tan^{-1}\left(\frac{y-y_1}{x-x_1}\right) \\ \tan^{-1}\left(\frac{z-z_1}{\sqrt{(x-x_1)^2 + (y-y_1)^2}}\right) \\ \tan^{-1}\left(\frac{y-y_2}{x-x_2}\right) \\ \tan^{-1}\left(\frac{z-z_2}{\sqrt{(x-x_2)^2 + (y-y_2)^2}}\right) \\ \frac{f^o}{c} \left( \frac{\vec{r}_2 \cdot \vec{v}_2}{\|\vec{r}_2\|} - \frac{\vec{r}_1 \cdot \vec{v}_1}{\|\vec{r}_1\|} \right) \end{bmatrix}. \quad (12)$$

where  $\Delta\tau'_{2,1}$  and  $\Delta f'_{2,1}$  are actual TDOA and FDOA values corresponding to the true aircraft location  $\mathbf{X}$ . The AOA profile representation within (12) is equivalent to the one shown in (10), and this equivalence can be easily derived from the

geometry of the problem shown in Fig. 4(a).

The noise vector can be represented as  $\eta = [\eta_{\Delta\tau_{2,1}}, \eta_{\phi_1}, \eta_{\theta_1}, \eta_{\phi_2}, \eta_{\theta_2}, \eta_{f_{2,1}}]^T$ . Thus the corresponding measured AOA-TDOA-FDOA profile can be represented as

$$\mathbb{M} = [\Delta\tau_{2,1}, \phi'_1, \theta'_1, \phi'_2, \theta'_2, \Delta f_{2,1}]^T,$$

where

$$\mathbb{M} = \Upsilon(\mathbf{X}) + \eta. \quad (13)$$

Let the noise covariance matrix be  $\chi = \mathbb{E}[(\eta - \mathbb{E}[\eta])(\eta - \mathbb{E}[\eta])^T]$ , where  $\mathbb{E}[\cdot]$  represents the expectation operator. In order to derive the GDOP it is essential to represent (12), in the form of Taylor series expansion [31],

$$\Upsilon(\mathbf{X}) \approx \Upsilon(\mathbf{X}_0) + \Upsilon'(\mathbf{X}_0)(\mathbf{X} - \mathbf{X}_0) \quad (14)$$

where  $\Upsilon'(\mathbf{X}_0)$  represents the derivatives matrix of dimensions  $6 \times 3$  evaluated at  $\mathbf{X}_0 = [x_0, y_0, z_0]^T$  for 2 sensor nodes within a 3D Cartesian co-ordinate system, and (14) can be represented as

$$\Upsilon(\mathbf{X}) \approx \Upsilon(\mathbf{X}_0) + \Gamma(\mathbf{X} - \mathbf{X}_0), \quad (15)$$

where  $\Gamma = \Upsilon'(\mathbf{X}_0)$  and

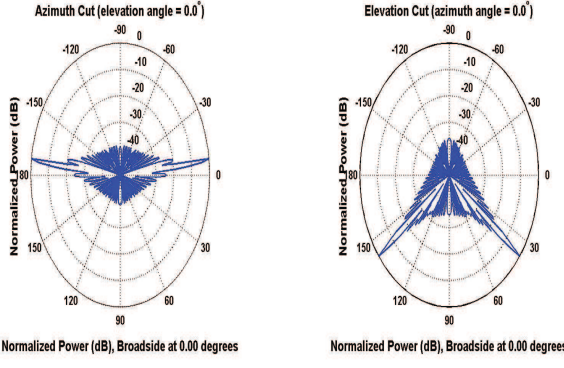


Fig. 7. Simulated beamforming pattern for 2D AOA estimate in Fig. 5(b) in azimuth and elevation.

$$\Gamma = \begin{bmatrix} \frac{\partial(\Delta\tau'_{2,1})}{\partial x}|_{\mathbf{x}_0} & \frac{\partial(\Delta\tau'_{2,1})}{\partial y}|_{\mathbf{x}_0} & \frac{\partial(\Delta\tau'_{2,1})}{\partial z}|_{\mathbf{x}_0} \\ \frac{\partial\phi_1}{\partial x}|_{\mathbf{x}_0} & \frac{\partial\phi_1}{\partial y}|_{\mathbf{x}_0} & \frac{\partial\phi_1}{\partial z}|_{\mathbf{x}_0} \\ \frac{\partial\theta_1}{\partial x}|_{\mathbf{x}_0} & \frac{\partial\theta_1}{\partial y}|_{\mathbf{x}_0} & \frac{\partial\theta_1}{\partial z}|_{\mathbf{x}_0} \\ \frac{\partial\phi_2}{\partial x}|_{\mathbf{x}_0} & \frac{\partial\phi_2}{\partial y}|_{\mathbf{x}_0} & \frac{\partial\phi_2}{\partial z}|_{\mathbf{x}_0} \\ \frac{\partial\theta_2}{\partial x}|_{\mathbf{x}_0} & \frac{\partial\theta_2}{\partial y}|_{\mathbf{x}_0} & \frac{\partial\theta_2}{\partial z}|_{\mathbf{x}_0} \\ \frac{\partial(\Delta f'_{2,1})}{\partial x}|_{\mathbf{x}_0} & \frac{\partial(\Delta f'_{2,1})}{\partial y}|_{\mathbf{x}_0} & \frac{\partial(\Delta f'_{2,1})}{\partial z}|_{\mathbf{x}_0} \end{bmatrix}. \quad (16)$$

The maximum likelihood estimate [32] for the aircraft position can be expressed as

$$\hat{\mathbf{X}} = \mathbf{X}_0 + (\Gamma^T \chi^{-1} \Gamma)^{-1} \Gamma^T \chi^{-1} [\mathbb{M} - \Upsilon(\mathbf{X}_0)]. \quad (17)$$

The covariance matrix for the position estimate is as shown in [32]

$$\mathbb{C} = (\Gamma^T \chi^{-1} \Gamma)^{-1}. \quad (18)$$

Thus from (18) the GDOP can be represented as  $\sqrt{(\text{Tr}[\mathbb{C}])}$ , where  $\text{Tr}[\cdot]$  represents the trace operator. Within  $k$  randomly deployed sensor nodes we intend to select the  $k'$  best sensor nodes which will minimize the GDOP. Let the optimal set of sensor node locations be represented as  $\mathbb{X} = [x_1, y_1, z_1, \dots, x_{k'}, y_{k'}, z_{k'}]$ . Let all the possible combinations of  $k$  sensor nodes among  $k$  randomly distributed sensor nodes be represented as  $\mathbb{S}$ .

The proposed GDOP minimization problem, which aims at appropriate selection of  $k'$  multilateration sensors positioned at  $\{x_1, y_1, z_1, \dots, x_{k'}, y_{k'}, z_{k'}\}$  can thus be presented as follows

$$\hat{\mathbb{X}} = \left[ \min_{\mathbb{X} \in \mathbb{S}} \sqrt{(\text{Tr}[\mathbb{C}])} \right]_{\hat{\mathbf{X}}_a}, \quad (19)$$

where  $[\cdot]_{\hat{\mathbf{X}}_a}$  represents the evaluation at the current aircraft position estimate generated after KF estimation using (11).

#### D. Conventional ADS-B based geolocation

We utilize the conventional ADS-B based geolocation to supplement our hybrid geolocation based approach. The geolocation estimate generated by this module would inform us

on the authenticity and the integrity of the ADS-B signal. If the ADS-B signal was spoofed or compromised, then there would be an obvious disagreement between the hybrid geolocation estimate and the estimate based on this conventional ADS-B frame demodulation. This module would thus serve to identify an attack or a message infringement on the ADS-B signal under consideration.

A typical ADS-B transmission frame is shown in Fig. 4(b). Within the data block, the pulse transmitted in the first half of the interval is a binary 1 and in the second half it is a binary 0. The preamble consists of 4 pulses, each having a duration of  $0.5 \pm 0.05 \mu\text{sec}$ . The second, third, and fourth pulses are spaced at 1, 3.5 and  $4.5 \mu\text{secs}$  respectively, as specified by [30]. The aircraft altitude, GPS position co-ordinates, barometric pressure, and heading can all be recovered by demodulating the ADS-B data block frame, as mentioned in [30]. The ADS-B demodulation block is responsible for relaying the demodulated ADS-B data pertaining to the aircraft's current location relative to the CU to serve as a back-up for the hybrid geolocation estimate.

#### IV. ADAPTIVE MODULATION AND BEAMFORMING

As described in the previous section, we obtain the real-time aircraft location estimation through the hybrid AOA-TDOA-FDOA mechanism and KF tracking. Based on this 3D geolocation estimate, we develop an adaptive modulation and beamforming strategy to facilitate the ATG communication. In this section, this adaptive modulation-beamforming framework is described in detail. We consider a direct dominant LOS path for the aircraft and the ground station for our analysis, which translates into a Rician channel [23], [24].

##### A. Adaptive Modulation

In order to ensure a good quality of service for applications like in-flight broadband ATG communications, it is vital to ensure that the Symbol Error Rate (SER) for the ATG channel should be minimized. With this objective, the proposed approach aims at selecting the best M-Phase Shift Keying (M-PSK) modulation, which ensures the target SER. This in turn depends upon the current real-time distance between the BS and the aircraft, received SNR  $\gamma$ , and channel conditions.

The received signal SNR can be represented as

$$\gamma = \frac{P_r}{N_o B} = \frac{P_t K_p \mathbb{E}[h]^2 (\frac{d_0}{d})^\beta}{N_o B} \quad (20)$$

where  $h$  is the channel gain,  $P_r$  is the received power,  $P_t$  is the transmitted power,  $K_p$  is the pathloss constant,  $N_o B$  is the noise power within bandwidth  $B$ ,  $d_0$  is the reference distance,  $d$  is the distance between the aircraft and the BS, and  $\beta$  is the path-loss exponent.

In [23] the authors derive an expression for SER under Rician channel as follows. The probability density function of the SNR at the receiver is given by

$$p(\gamma) = \left( \frac{1 + K_r}{m_\gamma} \right) \exp \left[ -\frac{(1 + K_r)\gamma + K_r m_\gamma}{m_\gamma} \right] I_0 \left( 2 \sqrt{\frac{K_r(1 + K_r)\gamma}{m_\gamma}} \right), \quad (21)$$

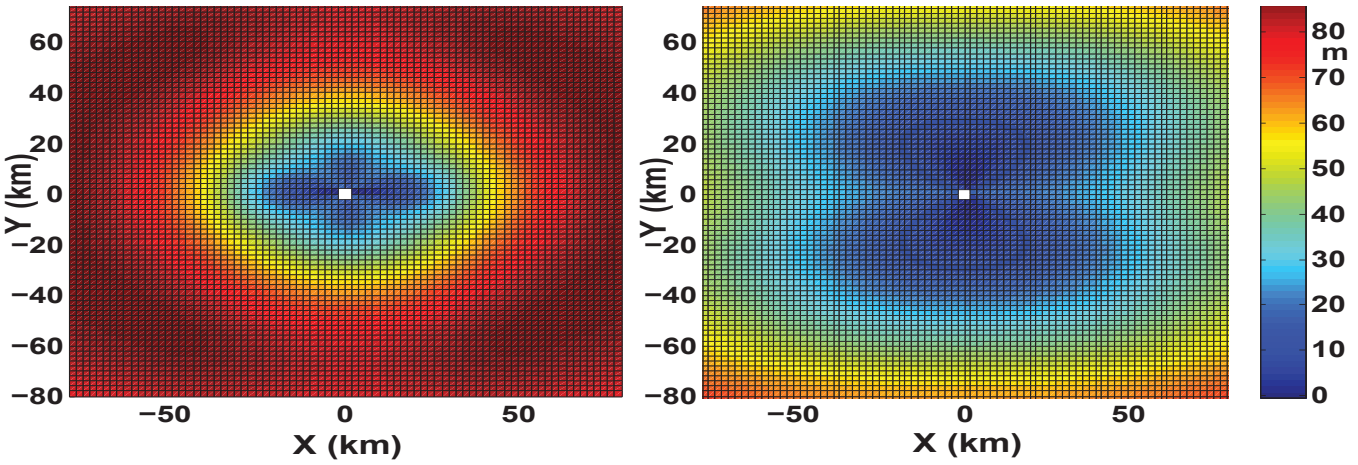


Fig. 8. Comparison between TDOA and hybrid AOA-TDOA-FDOA scheme.

where  $m_\gamma = \mathbb{E}[\gamma]$  is the average SNR,  $K_r$  is the Rician K-factor representing the ratio between the power in the direct path and the power in the other paths (in our case large  $K_r$  indicates that there exists a dominant LOS component) [33], and  $I_0(\cdot)$  is the zero order modified Bessel function of the first kind.

As shown in [23], the SER probability for M-PSK over Rician channel is given by

$$P_s(\xi) = \int_0^\infty P_s(\xi|\gamma)p(\gamma)d\gamma \quad (22)$$

The conditional probability of symbol error is given by

$$P_s(\xi|\gamma) = \frac{1}{\pi} \int_{-\pi/2}^{\pi/2} \exp\left[-\gamma \sin^2\left(\frac{\pi}{M}\right) \sec^2(\alpha)\right] d\alpha \quad (23)$$

Substituting (21) and (23) in (22), as shown in [23], we obtain,

$$P_s(\xi) = \frac{1}{\pi} \left( \frac{1+K_r}{m_\gamma} \right) \int_{-\pi/2}^{\pi/2} \frac{\exp\left(-\frac{K_r \sin^2\left(\frac{\pi}{M}\right) \sec^2(\alpha)}{\frac{1+K_r}{m_\gamma} + \sin^2\left(\frac{\pi}{M}\right) \sec^2(\alpha)}\right)}{\frac{1+K_r}{m_\gamma} + \sin^2\left(\frac{\pi}{M}\right) \sec^2(\alpha)} d\alpha \quad (24)$$

where  $M$  is the order of modulation within the M-PSK modulation scheme. In this work, we seek to achieve the target SER  $\leq T_{SER}$ , where  $T_{SER}$  is the SER threshold, by choosing the optimal  $M$ . The choice of  $T_{SER}$  depends on the ATG communication requirements to support the broadband service. The received SNR  $\gamma$  depends upon the distance of the aircraft from the BS and also depends upon the beamwidth gain available through beamforming. Depending upon the estimated value for  $\gamma$ , we solve (24) to find out the most optimum value for  $M$ .

Let the achievable SNR at the aircraft receiver  $\gamma$  be partitioned into  $N$  distinct levels such that  $\chi_i \leq \gamma \leq \chi_{i+1}$  for  $i = 0, \dots, N-1$  and  $\chi = \{\chi_i | i = 0, \dots, N; \chi_0 = 0; \chi_N \rightarrow \infty\}$  be the set over this achievable SNR partition.

The average throughput over this ATG channel,  $\mathbf{R}$  can be expressed as shown in [34],

$$\mathbf{R}(\gamma, \chi) = \mathbf{B} \left[ \sum_{i=0}^{N-1} \log_2 M(\chi_i) \int_{\chi_i}^{\chi_{i+1}} p(\gamma) d\gamma \right], \quad (25)$$

where  $M(\chi_i)$  is the modulation order chosen for the achieved SNR level  $\chi_i$ , this choice of  $M(\chi_i)$  is dictated by solving (24) for an optimal value of  $M$  to achieve SER  $\leq T_{SER}$ ,  $\mathbf{B}$  represents the bandwidth of the ATG communication channel.

### B. Beamforming

The received SNR  $\gamma$  can be improved by employing beamforming at the BS since we know the current real-time location and trajectory tracking through KF mechanism. In this work, we utilize the rectangular planar array operating at the aircraft communications channel to point the beam towards the real-time aircraft tracking estimate.

The rectangular array geometry is shown in [35]. We assume  $N_x$  and  $N_y$  number of isotropic antenna elements equally separated in  $X$  and  $Y$  directions by distances  $dx$  and  $dy$ . Let  $\phi$  and  $\theta$  be the desired azimuth and elevation angle for radiation. These angles can be easily deduced from the hybrid geolocation and AOA estimation shown in Section III-A and Section III-B. As shown in [35], the phase difference  $\varrho_{i,l}$  of element at  $(i, l)$ , relative to the element at  $(1, 1)$  chosen as reference, is given by

$$\begin{aligned} \varrho_{i,l} &= k_0(i-1)dx \sin(\theta) \sin(\phi) \\ &+ k_0(l-1)dy \sin(\theta) \cos(\phi), \end{aligned} \quad (26)$$

where  $k_0 = \frac{2\pi}{\lambda}$  represents the free space wave number. The resulting planar array radiation pattern  $\Omega(\theta, \phi)$  is given by

$$\Omega(\theta, \phi) = \Omega_e(\theta, \phi) \Omega_a(\theta, \phi) \quad (27)$$

where  $\Omega_e$  is the element radiation pattern  $\Omega_a(\theta, \phi)$  and the array radiation pattern can be expressed as

$$\Omega_a = \sum_{i=1}^{N_x} \sum_{l=1}^{N_y} w_{il} \exp [j(\varrho_{il})] \quad (28)$$

where  $w_{il}$  represents the complex weights of the individual elements so that the beam could be steered in the desired direction  $\{\theta_0, \phi_0\}$ , and can be represented as,

$$w_{il} = \exp \{-jk_0 [(i-1)dx \sin \theta_0 \cos \phi_0]\} \\ \times \exp \{-jk_0 [(l-1)dy \sin \theta_0 \sin \phi_0]\} \quad (29)$$

and the corresponding time delays  $\tau_{il}$  due to an impinging planar wavefront from direction  $(\theta, \phi)$  with respect to the reference element can be represented as,

$$\tau_{il} = -\frac{idx \sin \theta \cos \phi + ldy \sin \theta \cos \phi}{c} \quad (30)$$

where  $c$  is the velocity of light in free space.

#### **Algorithm 1** Adaptive ATG communication enabled by novel ADS-B based Multilateration.

- 
- ```

1: repeat
2:   | Capture ADS-B signal at randomly deployed  $k'$  multilateration sensors equipped with the UCA-AOA estimation hardware setup shown in Fig. 3(a).
3:   | At a particular multilateration sensor append a timestamp for the captured ADS-B frame by the GPS/rubidium enabled clock, compute the AOA and FOA for the received signal.
4:   | Relay the computed and captured data to the CU for geolocation, tracking and sensor selection feedback.
5:   | Collect the data from all the  $k'$  multilateration sensors and work out the position estimate for the aircraft through the hybrid AOA-TDOA-FDOA algorithm and ADS-B fusion by solving (11). Using standard KF as shown in [28], [29] estimate the track for the aircraft trajectory.
6:   repeat
7:     | Evaluate (19) for the most optimum  $k'$  sensor nodes among  $k$  sensors.
8:   | until GDOP minimization for current aircraft position estimate
9:   | Relay the computed tracking information to the ATG base station to enable adaptive modulation and beamforming as shown in Section IV.
10:  until Aircraft Trajectory Tracking

```
- 

## V. SIMULATION AND EXPERIMENTAL RESULTS

In this section, we discuss the simulation results based upon Algorithm 1 for the AOA-TDOA-FDOA based multilateration approach and the proposed adaptive beamforming-modulation scheme. In order to have realistic simulation parameters, we utilize the link budget parameters of ATG channels as mentioned in earlier works by Rice et. al [36]–[38] and other works like [39], [40], these parameters have been mentioned in Table I. The groupings of these parameters in Table I have been based upon various link ranges for air-to-air and air-to-ground channels. Also, the experimental result for evaluating the performance of hardware setup, shown in Fig. 3(a) for AOA estimation, is presented in this section.

### A. Performance Evaluation of the USRP based UCA-AOA Estimation Prototype

For the performance evaluation of the AOA estimation hardware setup, we use a fixed transmitter to generate the ADS-B signal at 1090 MHz at known location, which is spatially separated from the USRP based prototype shown in Fig. 3(a) and Fig. 3(b).

As shown in Fig. 3(a), the primary requirement for implementing the AOA estimation algorithms is to synchronize the receiver channels on three different levels: time synchronization, Analog to Digital Conversion (ADC) sampling or signal processing synchronization, and phase synchronization. As shown in Fig. 3(a), a clock distribution hardware unit, called Octoclock-G is used to synchronize the five USRP units in time. This unit provides 8 synchronized output reference clock frequencies at 10 MHz and synchronizes ADC and Field Programmable Gate Array (FPGA) processing at a rate of 1 pulse per second (PPS). However, phase synchronization remains a challenge because the frequency synthesizers are isolated on the RF board of each of the five individual USRPs. This results in the introduction of their individual random phase offsets, while the received signal is down-converted. To solve this problem, the frequency synthesizer output is drawn from a sixth reference USRP and is amplified by Low Noise Amplifier (LNA). This amplified output is then distributed among the five USRPs, which serves as an input to down conversion and ADC circuitry on each individual USRPs. This is achieved by modifying the WBX-RF daughter boards mounted on the USRP units. At the moment of activation of the UCA-AOA system, the Local Oscillator (LO) on the reference USRP locks onto a particular initial phase offset, and the remaining USRPs follow the same phase offset, and thus the phase synchronization is achieved. This phase synchronization approach directly affects the performance of the AOA estimation. The hardware implementation and prototype for achieving this prototype is shown in Fig. 3(a) and Fig. 3(b).

Fig. 5(a), in particular, shows the distribution of azimuth and elevation errors in over 600 real-time estimations of AOA from the acquired ADS-B signal. The ADS-B frame captured on the antenna array, is processed as described in the Section III-A, and the AOA of the signal is estimated using the hardware setup in Fig. 3(a). As we can see from this distribution plot, around 80% – 90% of the errors occur between 0 and 2 degrees in the real environment for both azimuth and elevation estimation. This performance evaluation was carried out by evaluating the error between true azimuth and elevation angles and those estimated by the AOA estimation setup described in Section III-A. The true angles are computed by identifying the latitude, longitude and altitude of the transmitter and the prototype setup, respectively by GNSS receivers placed at these two locations.

### B. Simulation Results

Fig. 5(b) represents the simulated UCA-RB-MUSIC algorithm result at a particular WAMLAT unit for estimation of azimuth and elevation angles for a simulated scenario. This 2D

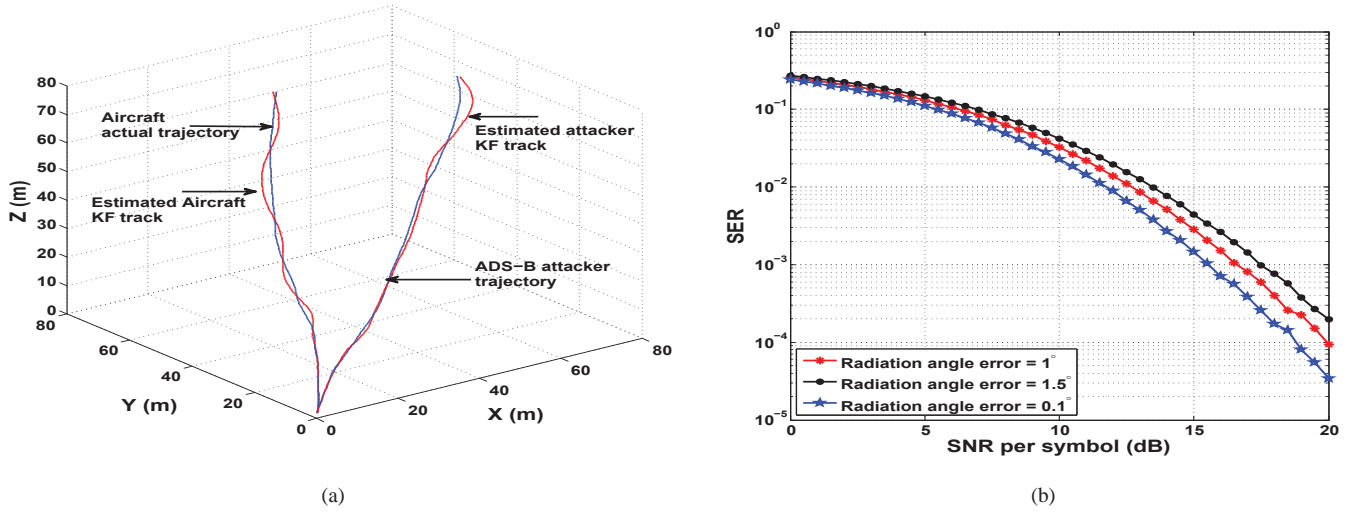


Fig. 9. (a) KF algorithm for tracking the aircraft trajectory, (b) Effect of radiation angle error on SER performance.

AOA estimate will be utilized by the adaptive beamforming mechanism within our simulation.

We assume several ground deployed WAMLAT units equipped with UCA, rectangular planar array to facilitate sharp beamforming, and ADS-B receiver modules synchronized by a GPS disciplined oscillator or a rubidium clock standard. In order to have realistic simulation parameters, we utilize the link budget parameters of ATG channels as mentioned in earlier works by Rice et. al [36]–[38] and other works like [39], [40]. The power of the ADS-B transponder on the aircraft is approximately 125 Watts for Class A1 ADS-B transponder [30], and an aircraft distance from the WAMLAT unit of 50 nautical miles (NM) or 92.6 km has been assumed in these simulations.

As mentioned earlier, the ADS-B signal is at 1090 MHz and we assume that the aircraft has ADS-B out capability. We assume a network of four WAMLAT units with a baseline separation of 20 NM between them. The ADS-B signal is captured over the antenna arrays on the WAMLAT units and this captured RF is sent to the 2D AOA estimation module and the ADS-B demodulation module as explained in Section III. The ADS-B demodulation module determines the identity of the aircraft and relays the captured ADS-B RF signal to the CU for computation of the hybrid geolocation.

Fig. 6(a) and 6(b) represent the AOA estimation accuracy for varying SNR levels, averaged over 100 simulations for each SNR value. Fig. 6(a) represents the RMSE error in AOA estimation at a particular WAMLAT unit. It should be noted that the AOA estimation algorithm achieves about  $0.5^\circ$  accuracy in estimation of the azimuth and elevation angle at  $\text{SNR} = 5 \text{ dB}$ . On the other hand, the UCA-ESPRIT algorithm as shown in Fig. 6(b) displays a much better AOA estimation accuracy of  $0.5^\circ$  within the lower SNR regime of around  $-8 \text{ dB}$ . However as shown in [25], the UCA-ESPRIT algorithm would require twice as many antenna elements

as the UCA-RB-MUSIC. This angle estimation is critical in deciding the radiation angle at the BS for enabling the ATG communication link. Fig. 7 represents the simulated beam-pattern upon the rectangular antenna array at a particular BS, with the beamforming weights as defined in (29). The radiation angle is corresponding to the AOA estimate generated by the UCA-RB-MUSIC algorithm as shown in Fig. 5(b). This sharp beamforming response pattern ensures a highly secure ATG communication link with the travelling aircraft.

Fig. 8 represents the 3D aircraft geolocation accuracy by the TDOA based approach and the AOA-TDOA-FDOA fusion based approach respectively. This RMSE in the aircraft geolocation was achieved through simulation by solving (11) for several aircraft positions within the 3D space around the BS. This result was interpolated between two consecutive aircraft locations and projected on to a 2D  $X - Y$  plane. As seen from Fig. 8, an accuracy of approximately 50 m could be achieved at a radial distance of 60 km from the BS. However, as seen from the Fig. 8, a much higher accuracy of approximately 25 m could be achieved through the proposed AOA-TDOA-FDOA based hybrid approach for a radial distance of 60 km to the aircraft.

In addition to this high accuracy geolocation the AOA-TDOA-FDOA framework is much more resilient to any ADS-B based attacks such as aircraft impersonation, spoofing, message infringement type attacks as discussed earlier in Section I.

Fig. 9(a) shows the performance of in-air ADS-B attacker discrimination against the actual aircraft trajectory. Even though the ADS-B message is spoofed by the nearby in-air attacker the hybrid geolocation scheme aided by the KF can effectively discriminate between the actual aircraft track and the trajectory of the attacker, with a resolution of the order of 50 m. Based on the *a priori* information on the actual flight path, actual aircraft trajectory can be

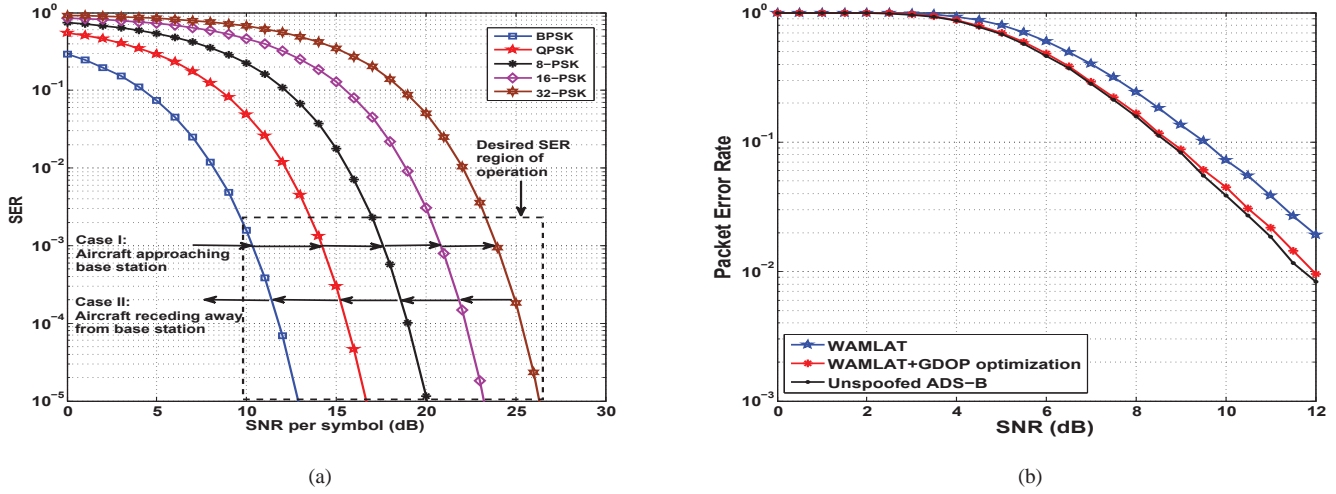


Fig. 10. (a) SER performance of the adaptive modulation-beamforming mechanism, (b) Packet error rate performance comparison.

distinguished from the attacker trajectory. The KF tracking RMSE performance demonstrates that we can achieve about 30 m tracking accuracy. This tracking estimate can be used for adaptive beamforming and modulation approach. As the error bound is of the order of 30 m between true trajectory and the estimated path, the SER performance with regards to the radiation angle error is acceptable as demonstrated in subsequent results.

Fig. 9(b) demonstrates the effect of the AOA estimation on the SER performance of the ATG system. If we are to use the AOA estimates from the hardware module, then we would be suffering an average estimation error of approximately  $1^\circ$  as shown in Fig. 5(a), this translates into a radiation angle for the ATG system, which will be offset by about 300 m at a distance of 10 NM or 18.5 Km. In Fig. 9(b) we can see that the SER performance is tolerant to this radiation angle offset and can still support a SER of approximately  $10^{-3}$  at SNR = 17 dB for a 8-PSK modulation scheme. However, as seen from Fig. 8, the proposed hybrid geolocation estimate is quite accurate in terms of localization error, thus it can be used to calculate the radiation angle more accurately than solely relying upon the AOA estimation module. These results were obtained by averaging over 50 iterations for each SNR value. These results prove that the proposed hybrid geolocation will provide better SER performance since the radiation angle offset will be significantly low.

Fig. 10(a) represents the adaptive modulation approach as discussed in Section IV. This plot shows the SER performance of various M-PSK schemes over a Rician channel with link range parameters as shown in Table I. The numerical value  $M$  is solved using (24) on order to ensure that we always obtain an SER less than a fixed target value of  $T_{\text{SER}} = 10^{-3}$ . The receiver at the aircraft is assumed to have an almost perfect knowledge of the channel, and performs maximum ratio combining in order to combine the beams from all the

BSs. Such a channel state estimation can be facilitated through training and pilot signals embedded within the transmission signal. The hybrid geolocation estimation at the BS, allows the BS to determine the SNR received and thus solve (24) in order to identify the best value for  $M$  in order to keep the SER below the target value. As we can see from Fig. 10(a), as the aircraft approaches the BS the estimated SNR improves and thus a higher value of  $M$  can be chosen and the exact opposite for a receding aircraft. These results were obtained by averaging over 50 iterations for each SNR value.

Fig. 10(b) demonstrates the effect of the proposed adaptive modulation and beamforming scheme on the packet error rate (PER) by utilizing the link range parameters as shown in Table I. We adopt a 1/2 rate convolutional encoding-Viterbi decoding, pilot training sequences to estimate the channel and maximal ratio combining at the uniform rectangular array at the ground based receiver. In particular, we assume a transmission time slot of  $T_s = 0.1$  msec with guard time  $T_g = 0.02$  msec, and assuming a expected link data rate of  $B = 10$  Mbps, the packet size should be  $L = B(T_s - T_g) = 800$  bits. The PER is then computed in relationship with the BER as  $\text{PER} = 1 - (1 - \text{BER})^L$ , where  $L$  is the packet size. Specifically we consider 3 cases for comparison, the proposed adaptive modulation and beamforming approach aided by, (i) AOA-TDOA-FDOA based WAMLAT approach, (ii) AOA-TDOA-FDOA based WAMLAT approach supported by GDOP based optimization, (iii) ADS-B based tracking, assuming we have un-spoofed ADS-B signal reception. The simulation result shown in Fig. 10(b) was obtained for a particular aircraft trajectory with 50 iterations for a particular SNR level.

For case (i), we utilize all the sensor nodes for computing the hybrid geolocation estimate and assuming that the ADS-B frame received is spoofed. The ATG system adopts adaptive modulation and beamforming based on this geolocation es-

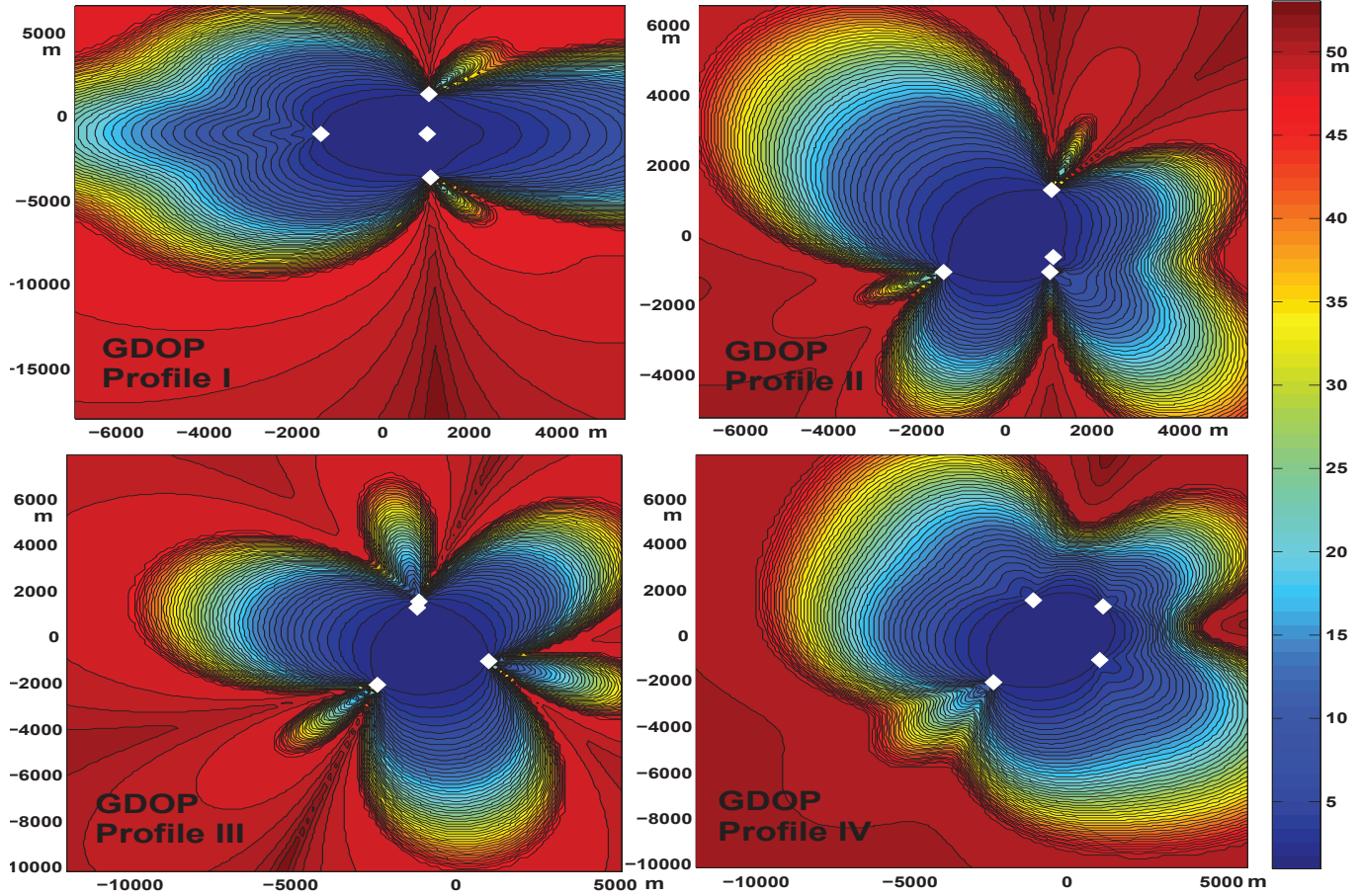


Fig. 11. Optimal Sensor selection through GDOP minimization.

timate and the Fig. 10(b) displays the achieved PER for this case. As seen from the plot, 10% PER is achieved at 9 dB SNR level, this performance is suboptimal when compared with the PER achieved by an accurate ADS-B signal aided geolocation. This performance degradation can be attributed to the dilution of precision in geolocation achieved by the WAMLAT approach due to suboptimal placement/selection of the sensor nodes. Case (ii) represents WAMLAT assisted by the proposed GDOP minimization based sensor selection. As seen from this simulation result, the SNR gain for achieving 10% PER is approximately 1 dB and matches the PER achieved by perfect ADS-B signal reception performance displayed in case (iii).

Fig. 11 represents the achievable GDOP profiles for the optimal selection of  $k' \in k$  sensor nodes, based on minimization of (19). The contour plots display the simulated GDOP that is achieved through the selection of  $k' = 4$  selected sensor nodes within  $k = 10$  sensor nodes for the latest estimated aircraft location. Fig. 11 represents GDOP profiles for 4 iterations of minimization within (19), GDOP profile IV represents the most optimal configuration or selection of  $k' = 4$  sensors. This GDOP profile selection for the current estimate of aircraft position, allows minimum dilution of precision and hence provides highly accurate AOA-TDOA-FDOA based geolocation estimate, in-spite of the fact that

the ADS-B message within the signal is corrupted. This high level of accuracy in geolocation of the aircraft translates to lower radiation angle error, and optimal modulation order selection by the ATG base station which in-turn results in higher beamforming gain in the direction of the aircraft and higher throughput for the overall communications system.

## VI. CONCLUSION

This work is focused on developing a novel WAMLAT strategy based on GDOP minimization for facilitating optimal sensor selection to strengthen the existing ATG communication framework. Specifically, this novel WAMLAT architecture adopts a hybrid geolocation mechanism to estimate the aircraft location coupled with an adaptive modulation and beamforming scheme for establishing a high data rate secure ATG communications link with the aircraft. Fusion of AOA and FDOA features with the conventional TDOA based geolocation alleviates the current security threats and vulnerabilities associated with the current ADS-B implementation. This refined hybrid geolocation estimate also assists in the development of *geolocation aided adaptive modulation and beamforming mechanism*, which facilitates a high fidelity ATG communications link between the BS and the aircraft. This novel WAMLAT strategy imparts two vital benefits, (i)

optimal selection of WAMLAT sensors in an attempt to reduce GDOP and enhance geolocation accuracy, which contributes in reduction of radiation angle error and corresponding quality of the ATG communications link, and (ii) this novel GDOP based WAMLAT strategy is resilient to ADS-B message infringement attacks, and provides accurate estimation for the aircraft location even if the ADS-B message is compromised. Our simulation results confirm the ability of the proposed system to achieve the same PER as an adaptive ATG communications system utilizing an “un-spoofed” ADS-B signal. Moreover our hardware based prototype offers a high performance solution to address the AOA estimation required within the hybrid geolocation mechanism. Actual field-trials with this novel hardware prototype demonstrate an accuracy of approximately  $1.5^\circ$  in the estimation of azimuth and elevation angles. This proposed integrated framework could also be extended for tactical communications involving fighter aircrafts to provide enhanced situational awareness and a secure ATG communications link.

## REFERENCES

- [1] E. Sakhaei and A. Jamalipour, “The Global In-Flight Internet,” *IEEE Journal on Selected Areas in Communications*, vol. 24, no. 9, pp. 1748–1757, Sept 2006.
- [2] J. Rasool, G. Oien, J. Hakegard, and T. Myrvoll, “On multiuser MIMO capacity benefits in air-to-ground communication for air traffic management,” in *6th International Symposium on Wireless Communication Systems, ISWCS 2009.*, Sept. 2009, pp. 458–462.
- [3] H. D. Tu and S. Shimamoto, “A Proposal of Wide-Band Air-to-Ground Communication at Airports Employing 5 GHz band,” in *IEEE Wireless Communications and Networking Conference, WCNC 2009.*, Apr. 2009, pp. 1–6.
- [4] D. Medina, F. Hoffmann, F. Rossetto, and C.-H. Rokitansky, “A Geographic Routing Strategy for North Atlantic In-Flight Internet Access via Airborne Mesh Networking,” *IEEE ACM Transactions on Networking*, vol. 20, no. 4, pp. 1231–1244, Aug. 2012.
- [5] G. McGrath, “An optimization metric for air-to-ground network planning,” *IEEE Transactions on Wireless Communications*, vol. 8, no. 5, pp. 2336–2340, May 2009.
- [6] A. Week, “Aviation week, intelligence network: Market briefing june 20, 2014.” [http://awin.aviationweek.com/portals/awin/cmsfiles/media/pdf/ad\\_pdf/2014/06/20/ad\\_06\\_20\\_2014.pdf](http://awin.aviationweek.com/portals/awin/cmsfiles/media/pdf/ad_pdf/2014/06/20/ad_06_20_2014.pdf), 2014.
- [7] G. in-flight services, “Hybrid solutions,” <http://commercial.gogoair.com/connectivity/technologies>, 2014.
- [8] ICAO, “Guidance Material: Security Issues Associated with ADS-B,” *International Civil Aviation Organization Asia and Pacific Office*, Sept. 2007.
- [9] H. You, Z. Hongwei, and T. Xiaoming, “Joint Systematic Error estimation algorithm for radar and Automatic Dependent Surveillance Broadcasting,” *IET Radar, Sonar Navigation*, vol. 7, no. 4, pp. 361–370, Apr. 2013.
- [10] J. Besada, A. Soto, G. de Miguel, J. Garcia, and E. Voet, “ATC Trajectory Reconstruction for Automated Evaluation of Sensor and Tracker Performance,” *IEEE Aerospace and Electronic Systems Magazine*, vol. 28, no. 2, pp. 4–17, Feb 2013.
- [11] C. Rekkas, “ADS-B and WAM deployment in Europe,” in *Tyrrhenian International Workshop on Digital Communications - Enhanced Surveillance of Aircraft and Vehicles (TIWDC/ESAV)*, Sept. 2011, pp. 35–40.
- [12] C. Reck, M. Reuther, A. Jasch, and L.-P. Schmidt, “ADS-B receivers with DOA estimation Independent surveillance broadcast 2014,” in *Tyrrhenian International Workshop on Digital Communications - Enhanced Surveillance of Aircraft and Vehicles (TIWDC/ESAV)*, Sept. 2011, pp. 219–222.
- [13] C. Reck, U. Berold, J. Weinzierl, and L.-P. Schmidt, “Direction of arrival estimation from secondary surveillance radar signals in presence of hardware imperfections,” in *European Radar Conference*, Oct. 2008, pp. 252–255.
- [14] C. Reck, U. Berold, J. Schur, and L.-P. Schmidt, “Direction of arrival sensor calibration based on ADS-B airborne position telegrams,” in *European Radar Conference*, Sept. 2009, pp. 77–80.
- [15] S. Jana and S. K. Kasera, “On Fast and Accurate Detection of Unauthorized Wireless Access Points Using Clock Skews,” *IEEE Transactions on Mobile Computing*, vol. 9, no. 3, pp. 449–462, Mar. 2010.
- [16] E. Valovage, “Enhanced ADS-B Research,” *IEEE Aerospace and Electronic Systems Magazine*, vol. 22, no. 5, pp. 35–38, May 2007.
- [17] R. Holdsworth, J. Lambert, and N. Harle, “Inflight Path planning replacing pure collision avoidance, using ADS-B,” *IEEE Aerospace and Electronic Systems Magazine*, vol. 16, no. 2, pp. 27–32, Feb. 2001.
- [18] A. Zeitlin and R. Strain, “Augmenting ADS-B with Traffic Information Service-Broadcast,” *IEEE Aerospace and Electronic Systems Magazine*, vol. 18, no. 10, pp. 13–18, Oct. 2003.
- [19] M. Strohmeier, M. Schafer, V. Lenders, and I. Martinovic, “Realities and challenges of nextgen air traffic management: the case of ADS-B,” *IEEE Communications Magazine*, vol. 52, no. 5, pp. 111–118, May 2014.
- [20] C.-H. Chen, K.-T. Feng, C.-L. Chen, and P.-H. Tseng, “Wireless Location Estimation With the Assistance of Virtual Base Stations,” *IEEE Transactions on Vehicular Technology*, vol. 58, no. 1, pp. 93–106, Jan 2009.
- [21] I. Sharp, K. Yu, and Y. Guo, “GDOP Analysis for Positioning System Design,” *IEEE Transactions on Vehicular Technology*, vol. 58, no. 7, pp. 3371–3382, Sept. 2009.
- [22] Symmetricom, “Rubidium Frequency Standard 8040C”. San Jose: Microsemi, 2011.
- [23] S. Jonqyin and I. Reed, “Performance of MDPSK, MPSK, and noncoherent MFSK in wireless rician fading channels,” *IEEE Transactions on Communications*, vol. 47, no. 6, pp. 813–816, Jun. 1999.
- [24] G. Wang, G. Chen, D. Shen, Z. Wang, K. Pham, and E. Blasch, “Performance evaluation of avionics communication systems with radio frequency interference,” in *IEEE/AIAA 33rd Digital Avionics Systems Conference (DASC), 2014*, Oct 2014, pp. 2A4–1–2A4–10.
- [25] C. P. Mathews and M. Zoltowski, “Eigenstructure techniques for 2-D angle estimation with uniform circular arrays,” *IEEE Transactions on Signal Processing*, vol. 42, no. 9, pp. 2395–2407, Sept. 1994.
- [26] E. Research, “USRP N210, WBX and Octoclock data sheet,” <https://www.ettus.com>, 2014.
- [27] H.-J. Du and P. Y. Lee, “Simulation of Multi-Platform Geolocation using a Hybrid TDOA-AOA Method,” *Technical Memorandum Defense R and D Canada*, Dec. 2004.
- [28] J. da Silva, J. Brancalion, and D. Fernandes, “Data fusion techniques applied to scenarios including ADS-B and radar sensors for air traffic control,” in *12th International Conference on Information Fusion, 2009. FUSION '09*, July 2009, pp. 1481–1488.
- [29] K. Yoo, D. Won, S. Sung, and Y. J. Lee, “Hybrid tracking of maneuvering multiple-aircraft in 3d space,” in *ICCAS-SICE, 2009*, Aug 2009, pp. 3239–3244.
- [30] R. inc, “Minimum Operational Performance Standards (MOPS) for 1090 MHz Automatic Dependent Surveillance-Broadcast (ADS-B),” *RTCA DO-260*, vol. 1, no. 1, Sept. 2000.
- [31] Y. Xue, X. Li, L. Xu, and Y. Ren, “Research on position differential method of dual-satellites TDOA and FDOA in passive location system,” in *IEEE International Frequency Control Symposium (FCS), 2012*, May 2012, pp. 1–5.
- [32] D. Torrieri, “Statistical Theory of Passive Location Systems,” *IEEE Transactions on Aerospace and Electronic Systems*, vol. AES-20, no. 2, pp. 183–198, March 1984.
- [33] E. Haas, “Aeronautical channel modeling,” *IEEE Transactions on Vehicular Technology*, vol. 51, no. 2, pp. 254–264, Mar. 2002.
- [34] H.-P. Lin, M.-C. Tseng, and D.-B. Lin, “Performance analysis of Mary PSK adaptive modulation system over Rayleigh-lognormal fading channel,” in *IEEE 61st Vehicular Technology Conference*, vol. 1, May 2005, pp. 576–580.
- [35] O. Manu, M. Dimian, and A. Graur, “Analysis of Beamforming in Phased Antenna Arrays,” in *10th International Conference on Development and Application Systems, Suceava, Romania, May 27–29, 2010*, May 2010.
- [36] A. G. Longley and P. L. Rice, “Prediction of tropospheric radio transmission over irregular terrain, a computer method-1968,” *ESSA Tech. Rep. ERL 79-ITS 67*, U.S. Government Printing Office, Washington, DC, July 1968.
- [37] P. L. Rice, A. G. Longley, K. A. Norton, and A. P. Barsis, “Tech note 101: Transmission loss predictions for tropospheric communication circuits,” *U.S. Government Printing Office, Washington, DC, NBS Tech. Note 101*, May 1965.
- [38] G. A. Hufford, A. G. Longley, and W. A. Kissick, “A guide to the use of the its irregular terrain model in the area prediction mode,” *NTIA Report*, pp. 82–100, Apr. 1982.

- [39] B. Smida and V. Tarokh, "Ground-to-air interference analysis in cellular ATG systems," in *42nd Annual Conference on Information Sciences and System, CISS 2008*, Mar. 2008, pp. 225–228.
- [40] T. Almond and J. Clarke, "Consideration of the usefulness of microwave propagation prediction methods on air-to-ground paths," *IEE Proceedings For Communications, Radar and Signal Processing*, vol. 130, no. 7, pp. 649–656, Dec. 1983.



**Yogesh Anil Nijssure** received the B.E. degree (Distinction) in Electronics Engineering from University of Mumbai, India, in June 2006 and received his M.Sc. degree (Distinction, Rank 1) in Wireless Communication Systems Engineering from the University of Greenwich, U.K. in September 2008. He received his Ph.D. degree from University of Newcastle upon Tyne in U.K. in October 2012. From March 2010 to September 2010 he undertook his research internship at the Institute for Infocomm Research (I2R), Singapore, as a research engineer. From November 2011 to November 2012 he worked as a Research Associate at Nanyang Technological University, Singapore. From December 2012 to April 2014, he undertook research within the aerospace industry. Since April 2014, he is working as a postdoctoral research fellow at Ecole de technologie supérieure (ETS), University of Quebec located in Montreal, Canada. His research interests include cognitive radar network design, Bayesian non-parametric methods, UWB radar systems, robust ADS-B multilateration systems, cognitive radio networks, information theory, radar signal processing, electronic warfare and software defined radio systems.



**Georges Kaddoum** is an Assistant Professor of Electrical Engineering at Ecole de technologie supérieure (ETS), University of Quebec located in Montreal, Canada. Dr. Kaddoum received his bachelor degree in Electrical Engineering from ENSTA-Bretagne (Ecole nationale supérieure de techniques avancées) and M.S. degree in Telecommunications and Signal Processing (circuits, systems & signal processing) from the Université de Bretagne Occidentale and Telecom Bretagne (Brest, France) in September 2005. In December 2008, he earned his

Ph.D. degree in signal processing and telecommunications with honor from the National Institute of Applied Sciences (INSA), University of Toulouse. He was a scientific researcher at ETS in 2012 and then promoted as an assistant professor in November 2013. In 2014, he was awarded the ETS research chair in physical layer security for wireless networks. In addition, Prof. Kaddoum was also a recipient of the Best Paper Award at the IEEE International conference Wireless and Mobile Computing, Networking and Communications (WiMob 2014) with three other coauthors. His recent research activities cover wireless communication systems, chaotic modulations, secure transmissions, and space communications & Navigation. He has published over 60 journal and conference papers and has held two pending patents. Since 2010, Prof. Kaddoum has been working as scientific consultant in the field of space and wireless telecommunications for with several companies (Intelcan Technosystems, MDA Corporation and Radio-IP companies).



**Ghyslain Gagnon** received the B.Eng. and M.Eng. degrees in electrical engineering from cole de technologie supérieure, Montreal, Canada in 2002 and 2003 respectively. He also received the Ph.D. degree in electrical engineering from Carleton University, Canada in 2008. From 2003 to 2004, he worked for ISR Technologies where he designed and implemented several critical synchronization modules for a software defined radio which later obtained the editors' choice award in 2007 by the portable design magazine. He is now an associate professor with the department of Electrical Engineering, cole de technologie supérieure. He is inclined towards industrial research partnerships. His research aims at mixed-signal circuits and systems, as well as digital signal processing.



**FRANOIS GAGNON** (S87M87SM99) received B.Eng. and Ph.D. degrees in electrical engineering from cole Polytechnique de Montréal. Since 1991 he has been a professor with the Department of Electrical Engineering, cole de Technologie Supérieure. He chaired the department from 1999 to 2001, and now holds the NSERC Ultra Electronics Chair, Wireless Emergency and Tactical Communication, at the same university. His research interest covers wireless high-speed communications, modulation, coding, high-speed DSP implementations, and military point-to-point communications. He has been very involved in the creation of the new generation of high-capacity line-of-sight military radios offered by the Canadian Marconi Corporation, which is now Ultra Electronics Tactical Communications Systems. The company has received, for its product, a "Coin of Excellence" from the U.S. Army for performance and reliability. He was awarded the 2008 NSERC Synergy Award (Small and Medium-Sized Companies category) for the fruitful and long lasting collaboration with Ultra Electronics TCS.



**Dr. Chau Yuen** received the BEng and PhD degree from Nanyang Technological University (NTU), Singapore, in 2000 and 2004 respectively. Dr Yuen was a Post Doc Fellow in Lucent Technologies Bell Labs, Murray Hill during 2005. He was a Visiting Assistant Professor of Hong Kong Polytechnic University in 2008. During the period of 2006-2010, he worked at the Institute for Infocomm Research (I2R, Singapore) as a Senior Research Engineer, where he was involved in an industrial project on developing an 802.11n Wireless LAN system, and participated actively in 3Gpp Long Term Evolution (LTE) and LTE-Advanced (LTE-A) standardization. He joined the Singapore University of Technology and Design as an assistant professor from June 2010, and received IEEE Asia-Pacific Outstanding Young Researcher Award on 2012. Dr Yuen serves as an Associate Editor for IEEE Transactions on Vehicular Technology, and awarded as Top Associate Editor from 2009 - 2014. He has 2 US patents and published over 200 research papers at international journals or conferences.



**Rajarshi Mahapatra** received his Ph.D in Electronics and Communication Engineering from IIT Kharagpur. Recently, he has completed his Postdoc in CEA-LETI, France. In his postdoc research, he was engaged in FP7 Call4 BeFEMTO and Green-touch. He is currently working as Professor in the Dept. of ECE, Graphic Era University, Dehradun. He has served as a member of TPC for several national and international conferences and peer-reviewed journals in the area of wireless network. He has published about 20 peer reviewed paper in several international journals and conferences. His current research interests include cognitive radio, dynamic spectrum access, energy consumption in wireless networks and optical access networks.